JOURNAL OF OPTOELECTRONICS AND ADVANCED MATERIALS, Vol. 11, No. 4, April 2009, p. 399 - 407

Effect of Bi addition on Se-Te chalcogenide system

NIKHIL SURI*, P. K. KHANNA
Hybrid Microcircuit Group, Central Electronics Engineering Research Institute (CEERI)/ Council of Scientific and Industrial Research (CSIR), Pilani-333031 (Rajasthan) India

The effect of Bi addition on Se-Te system has been presented. On the basis of obtained results a bright future for these materials has been predicted. Bismuth has a unique property of p to n type conversion. A lot of information is gathered from the present work but a lot more can be done for more detailed understanding of the selected system.

(Received April 6, 2009; accepted April 23, 2009)

Keywords: Amorphous Chalcogenides, Glass Transition, Crystallization, Thermal stability

1. Introduction

Science is not conducted by brains and hands but by individuals as H. Fritsche said. The whole activity of many intelligent men and women developed the field of glassy and amorphous chalcogenides up to the bright level of today. Chalcogenide (lone pair semiconductors) can be either elemental semiconductors such as S, Se etc., binary such as As_2S_3, As_2Se_3 etc., multicomponent mixture as Si-Ge-Te-As, As_2S_3:Tl_2Se_3 etc. The elemental or binary chalcogenides have chain or layered structure with considerable order extending locally in one or two dimensions whereas, multicomponent alloys possess 3-D network. The understanding of electronic states in the Chalcogenide glasses is still not complete. The absence of rigidity of the structure in Chalcogenide glasses make them suitable for several applications.

Chalcogenide materials obey so-called '8-N bonding rule' proposed by Mott [1] according to which all electrons are taken up in bonds so that large changes of conductivity with small changes of composition do not occur. These materials find vast applications as optical fibers, memory devices, reversible phase change optical recording materials etc. [2-3]. All these glasses have good mechanical properties such as hardness, adhesion, low internal stress and water resistance. They are used as core materials for optical fibers for transmission in the wavelength range of 6–12 μm, especially when short lengths and flexibility are required [4]. Selenium is mostly used because of its wide commercial importance. Its device applications such as rectifiers, photocells and switching memory have made it attractive. Adding a second element to Selenium improves the corrosion resistance property of Selenium [5] and these alloys are promising media for phase change recording devices. Tohge and co-workers [6, 7] and Nagels et al. [8, 9] have shown that the addition of Bi atoms to chalcogenide glasses produces a remarkable change i.e., from p- to n type conduction, while addition of other elements of group V (Sb, As) always yields p-type conduction. The aim of our work was to study the effect of Bi atoms on the electrical and optical properties of a Se-Te matrix.

The first paper that dealt with the addition of Bismuth in chalcogenides was published by Bowman and Schotmiller in 1968. Schotmiller et al. have shown that the Bismuth addition to certain chalcogenides (e.g., Ge-Se chalcogenides) changed the carrier type from p-type to n-type [10]. Bi appears to be unique in this regard, for example, the addition of other group V elements, such as P, As or Sb does not alter the dominant carrier type. Wang et al. [11] studied the effect of Sn and Bi addition on the properties and structure of Ge-Se-Te chalcogenide glass by X-ray diffraction, differential thermal analysis (DTA), IR transmission spectra and far-Fourier transform infra-red (FTIR) spectra to expand the IR transparency region of the Ge-Se-Te glasses. The addition of Sn atom increased the T_g, crystallization temperature (T_c), anti-crystallization stability, chemical durability and IR multiphonon edge. The addition of Bi increased the chemical durability and broadens the IR transparency region. Influence of composition on the electrical and optical properties of $Ge_{20}Bi_xSe_{80-x}$ films have been studied by Zahed et al. [12]. They measured the optical gap and electrical resistivity of a series of $Ge_{20}Bi_xSe_{80-x}$ glasses (x = 0, 5, 9, 10, 15, 20, 25). They analyzed the absorption spectra of films with different Bi compositions to determine the optical band gap. They found that the optical band gap decreases sharply from 2.1-1.65 eV as the Bi content increased to 10 at. %. A slight change has been observed for Bi > 10 at. %. A large decrease in the electrical activation energy from 0.97-0.09 eV occurred as the Bi content is increased up to 10 at. %. The optical and electrical data suggest that the addition of Bi produces localized states near the conduction-band edge, so the electrical transport is due to hopping of electrons after being excited into localized states at the conduction-band edge. An increasing number of paper have been reported in literature dealing with various properties of Bi-containing Chalcogenides bulk glasses for the most part Ge-chalcogen (S, Se, Te) alloys. Electrical properties such as conductivity, thermopower, optical properties have been extensively studied as

function of both composition and temperature and also of pressure by various researchers [12-17]. Agnihotri et al. by study of X-ray K absorption edges of Se and Ge in $Ge_{22}Se_{78-x}Bi_x$ showed that low concentration of Bi, forms Bi-Se bonds, while at high concentration Ge-Bi bonds are favoured [18-19]. Elliot et al. [20] in their paper on EXAFS study concluded that coordination number of Bismuth for all the contents is 3 ruling out all the assumptions of 4 and 6. Elliot and Steel studied the structural environment of Bi in $Ge_{20}Bi_xSe_{80-x}$ for $3 \leq x \leq 10$ using Extended X-ray absorption fine structure [EXAFS] microscopic information.

Usually, there is a decrease in the optical gap (E_{opt}^{g}), DC activation energy (ΔE) with alloying or doping. Sometimes, ΔE decreases more rapidly than E_{opt}^{g}, may be due to the change in E_{opt}^{g} and the valence-alternation pair energies with alloying. The Fermi energy level is quite effectively pinned by the valence-alternation centres. However, the presence of charged additive greatly reduces this pinning effect [21]. The role of defects in carriers type reversal on doping Ge-Se glasses with Bi using photoluminescence spectroscopy has been studied by Bhat et al. [22] for the systems $Ge_{20}Se_{100-x}Bi_x$ and $Ge_{20}Se_{70-x}Bi_xTe_{10}$. The composition at lower Bi content exhibited luminescence, while the composition showing n-type conduction failed to exhibit it. Bi addition has been observed to bring about a relative diminishing in D^+ as compared to D^- ones.

2. Experimental Procedures

2.1 Preparation of bulk material

Bulk samples of $Se_{80-x}Te_{20}Bi_x$ ($0 \leq x \leq 8$) were prepared by conventional melt quenching technique [23-25]. The exact proportion of high purity elements (99.999%), Sigma-Aldrich USA, in accordance with their atomic percentages was weighed using an electronic balance (Sartorious; model no. GC1603S-OCE). Materials were sealed in cleaned and evacuated glass ampoule (length~5 cm and internal diameter of 0.8 cm) in the vacuum of 10^{-5} mbar. The ampoule cleaning involves following methods: aqua regia (1 part of Nitric Acid+3Parts of HCl) cleaning, HF cleaning, Distilled water cleaning, acetone cleaning, ultrasonic cleaning and finally dries in oven for 2-3 hrs. It was recognized that Se has high vapor pressure and high tendency to react with oxygen. Thus, care and precaution were taken to avoid any explosion during the sealing of the tube. The sealing of the tube was done with utmost care in high vacuum. The ampoule was kept inside the vertical furnace and the temperature was raised to 1123 K slowly (3-4 K/min) and maintained there for 48 hrs. The ampoule was inverted at regular intervals of time to ensure homogeneous mixing of the constituents. It was then quenched in ice cold water. The material was separated from quartz ampoule by dissolving it in $HF+H_2O_2$ solution for about 48 hrs. The obtained ingot in this manner was of ~2 cm long and ~0.8 cm in diameter. The obtained ingot is powdered in motor pessel and the powdered material is used for further characterization.

2.2 Thin films

Thin films are very important by technological point of view. Thin films can be prepared by different methods viz., vacuum evaporation [26-29], electron beam evaporation [30], flash evaporation [31], RF sputtering [32], ion beam evaporation [33], chemical bath deposition [34], chemical vapour deposition and plasma-enhanced chemical vapour deposition [35-36] etc. Electrical, photoelectrical and optical properties of thin films are highly dependent on prevailing deposition methods.

In this work thermal evaporation method is used to grow the thin films of Bismuth doped Se-Te system. The substrates used for depositing thin films were properly cleaned Corning glass slides. Due to the presence of the foreign material on the substrates like oil or grease film may peel and there may be the possibility of formation of pinholes. Cleaning of the slides can be done by similar way as explained earlier for ampoules. Cleanliness of the films plays a major role and hence it is one of the utmost important parts of the thin film growing process. These cleaned substrates are placed in the Hind High Vacuum Coating Unit (model 12A4D) directly above the boat so that vapors of the material are deposited on them. The molybdenum boats are used to grow the thin films. The coating chamber is cleaned with acetone prior to each deposition. The thickness of the films was found to be ~2300 Å for all the samples. Talysurf (Taylor Hobson: model 2015) was used to measure the thickness of the films. These films were used to make all necessary electrical measurements.

3. Characterization of Se-Te: Bi

The prepared material can be characterized by number of ways viz., content analysis of the material is done my Kasap et. al using an Elan Inductively coupled Plasma Mass spectrometer (ICP-MS). The thermal studies of the system can be done by using Differential Scanning Calorimetry [37].

3.1 Structure and composition

The amorphous nature of the bulk and thin film can be verified by taking XRD scans by using X-Ray diffraction technique (Model: Philips PW1610, Goniometer: Philips1710, detector Cu-K_α. In XRD, each atom becomes the source of scattered X-ray radiation. The scattered radiation from all the atoms of glassy material will combine destructively as they fall on top of one another in the random manner. However, in the case of perfect crystal, the X-rays scatter without the loss of energy and

constructive interference may occur. XRD pattern was obtained using Cu-K_α radiations. Absence of prominent peaks confirmed the amorphous nature of the bulk and thin films. The composition of the thin film was analyzed by electron probe microanalysis (EPMA) using JEOL JXA 8600 M superprobe with accelerator voltage 15 keV, with probe diameter 5μm and probe current 50 nA.

3.2 Thermal studies

Thermal studies can be done by the Differential Scanning Calorimetry (DSC) and the thermal parameters can be easily and accurately obtained by it. The DSC monitors heat effects associated with phase transitions and chemical reactions as a function of temperature. In a DSC the difference in heat flow to the sample and a reference at the same temperature, is recorded as function of temperature. Calorimetric studies were done on bulk $Se_{80-x}Te_{20}Bi_x$ (x = 0.0, 0.2, 0.5, 1.0, 1.5, 2, 4, 6, 8) using Mettler Toledo Star^e DSC system. Calorimetric studies performed under non-isothermal conditions at different heating rates 5, 10, 15 and 20 $Kmin^{-1}$ respectively. The DSC equipment was calibrated with standard materials prior to the start of the experiment. 25 mg of powdered sample were crimped into aluminium pans and scanned at continuous heating rates (α = 5, 10, 15 and 20 K min^{-1}). All DSC runs were performed under the liquid nitrogen atmosphere. In all the scans we get three peaks, first endothermic peak is glass transition temperature (T_g), next exothermic peak is crystallization temperature (T_p) and the third one is melting temperature peak ™.

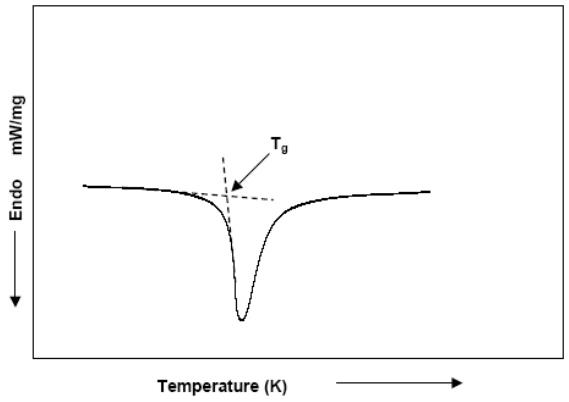

Fig.1 DSC trace indicating determination of T_g

The glass transition temperature is defined as the temperature corresponding to the intersection of two linear portions adjoining the transition elbow of DSC trace of first endothermic peak as shown in Fig. 1. The T_c is taken as the temperature corresponding to the onset of crystallization. The fraction X crystallized at temperature T is calculated as $X = A_T/A$, where A_T is the area of the exotherm between T_c and T and A is the total area of the exotherm (Fig. 2). The apparent activation energies of glass transition and crystallization have been calculated from the heating rate dependence of T_g and T_p respectively. The glass forming ability of the system calculated is very important and this is the area which is steadily evolving.

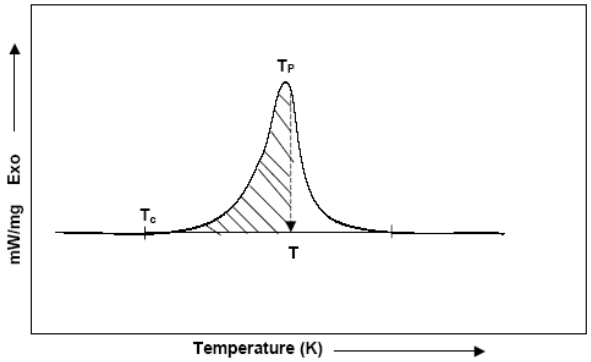

Fig. 2 Typical DSC crystallization exotherm for calculating volume fractions of precipitated crystals.

3.3 Optical studies

The normal incidence transmission spectrum has been measured by a double beam UV/VIS/NIR computer-controlled spectrophotometer (Shimadzu, Japan) in the wavelength range of 300-1100nm. The absorption coefficient, α, was calculated using the relation

$$\alpha = \frac{1}{t} \times \ln\left(\frac{100}{T'}\right) \quad (1)$$

where t is the thickness of the films and T' is the percentage transmission.

The optical band gap (E_{opt}^{g}) was obtained by taking the intercept on the energy axis in the $(\alpha h\nu)^{1/2}$ versus ($h\nu$) plot [38].

3.4 DC conductivity setup

The sample holder used to mount the samples is shown in a schematic diagram (Fig. 3). It consists of a copper base, on which thin film sample was mounted. A Pt-100 thermocouple was placed very near to the sample to record the temperature of the sample. A micro-heater was attached to the copper base plate to vary the temperature of the sample. Thin copper wires were used as leads of electrodes, which were connected to the electrodes with silver paint in order to make a good electrical contact. Liquid nitrogen was used as coolant for low temperature conductivity measurements. The dc

conductivity of the films was calculated by using following relationship.

$$\sigma = \frac{l \times I}{A \times V} \Omega^{-1} \text{cm}^{-1} \quad (2)$$

Where l is the electrode gap, A is the area of cross section and is given as $A = t \times w$, t is thickness and w is the width of the thin film respectively, I is the current flowing through the sample and V is the voltage applied to the electrode of the samples.

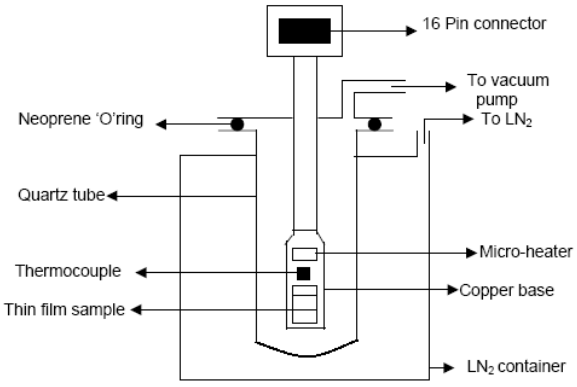

Fig. 3 Schematic diagram of conductivity set-up.

3.5 Electrical studies

Dark and photoconductivity studies have been done on the temperature range of 253-333 K. All the electrical measurements were done in the running vacuum of 10^{-5} mbar. Electrical contacts were made on the thin films using silver paint electrodes in a coplanar geometry (length 0.9 cm and gap between electrodes 0.3 cm) for all the samples. During photoconductivity studies the electrodes were well covered using aluminium foil, so that photo-diffusion did not take place. The sample was mounted inside a metallic cryostat with a transparent window. For photoconductivity measurements, the samples were illuminated using a tungsten halogen lamp (Halonix, India) of 500 W. Infrared filters were used to avoid the heating of the samples. The intensity of light was measured with a digital lux meter (LX-101, Taiwan). The photocurrent was measured using a digital picoammeter (DPM-111 Scientific Equipments, Roorkee).

3.6 Annealing studies

Thermal annealing of $Se_{80-x}Te_{20}Bi_x$ ($2 \leq x \leq 8$) samples has been done well below glass transition temperature in the bell jar of the vacuum system in the running vacuum of 10^{-5} mbar with heater fitted inside. The digital temperature controller with a power supply was used to control the temperature at the sample. The thin films grown by thermal evaporation method were annealed in high vacuum of the order 10^{-5} mbar. Electrical and optical studies were carried out on annealed samples. The data of annealed and pristine samples were compared in optical as well as electrical measurements.

4. Results & discussions

4.1 Structure and composition

The bulk and thin films of the amorphous samples have been characterized for their amorphous nature using the X-ray diffraction method. No sharp peaks in the diffractograms indicate the amorphous nature of the films. EPMA studies have shown that the actual compositions of the elements in thin films differ from that of bulk glass by about 3%, 4% and 1% for bismuth, tellurium and selenium, respectively.

4.2 Thermal Studies

In the present section attempt has been made to analyze the effect of Bi on thermal properties of Se-Te system. In Kasap et. Al. paper they investigated both heating and cooling schedules. $Se_{80-x}Te_{20}Bi_x$ ($0 \leq x \leq 8$) system has been studied under non-isothermal conditions at different heating rates 5, 10, 15 and 20 K min^{-1}. From the heating rate dependence of glass transition temperature (T_g) and peak crystallization temperature (T_p), the apparent activation energy for glass transition and activation energy for crystallization have been investigated. The thermal stability factor and the glass forming tendency of $Se_{80-x}Te_{20}Bi_x$ have also been investigated.

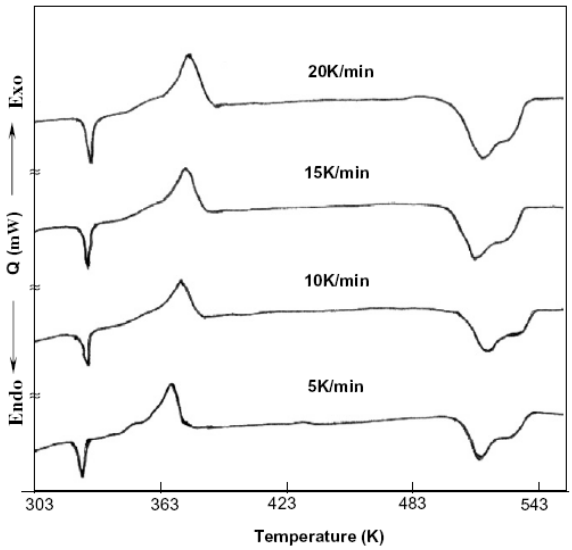

Fig. 4 DSC thermograms of $Se_{79}Te_{20}Bi_1$ at different heating rates

DSC thermograms for $Se_{80-x}Te_{20}Bi_x$ (x = 1.0) are shown in the Fig. 4. It can be seen from the figure that T_g

and T_p shifts towards higher temperature with increase in heating rate. Samples with other values of x also show similar behavior. The glass activation energy is the amount of energy that is absorbed by a group of atoms in the glassy region so as to jump from one metastable state to another [39]. In other words, the activation energy is involved in the molecular motions and rearrangements of the atoms around the glass transition [40]. In the system under study the glass transition temperature was found to increase with increase in heating rate as well as with increase in Bismuth concentration. This increase in the value of T_g with Bismuth content can be explained with the help of chemically ordered network (CON) model according to which the heteropolar bond is favoured over the homopolar bond. This explains the increase in T_g with the increase in Bi content. When the sample is reheated in the DSC furnace, the atoms undergo infrequent transitions between the local potential minima separated by different energy barriers in the configuration space where each local minimum represents a different structure. The most stable local minimum in the glassy region has lower internal energy. Accordingly, the atoms in a glass having minimum activation energy have a higher probability to jump to the metastable state (or local) of lower internal energy and hence is the most stable [39]. Therefore, one can argue that the addition of Bi reduces the stability of the glasses under investigation. A plot of glass transition temperature (T_g) versus the heating rate (α) is shown in Fig. 5. In all the samples T_g obeys the empirical relation.

$$T_g = A + BLog(\alpha) \tag{3}$$

where A and B are constants. The value of B is calculated from the slope of T_g vs. log (α) plots. The change in B with Bi concentration indicates that the Se-Te-Bi alloy undergoes structural changes with Bi addition [41]. The apparent activation energy for glass transition E_t is calculated using the Kissinger formula [3, 42] and the values of apparent activation energy (E_t) for glass transition for all the samples, obtained from their slopes are listed in the Table 1. Activation energy for crystallization is calculated from the modified Kissinger equation [3, 43-44]. The activation energy for crystallization has been calculated by using the expression given by Matusita et al. [45]. The value of m & n depending on the morphology of the growth is taken as m = n-1 if there is no previous heat treatment and m = n if the sample undergone a heat treatment [46]. In the present case no heat treatment was given, however, the presence of an endothermic peak indicates that a thermal relaxation has taken place. Also, due to the lower value of the T_g, it can be reasonably assumed that the sample might have undergone a heat treatment at room temperature. Hence, the value of m is taken as equal to n in the present case for further analysis. The values of both m and n are reported in Table 1. The values of E_c calculated from different methods show similar behavior but a discrepancy in the values of E_c evaluated may be attributed to the different approximations that have been adopted while arriving at the final equation. In addition the, pressure and temperature gradients in the sample (resulting from heat effect e.g. heating rate) vary randomly and such random variations have predominant effects on kinetic parameters. Hence, the variation in the value of E_c is expected to occur in the light of the reasons mentioned above. Similar variations in the activation energy have also been observed in the case of LiO_2-$2SiO_2$ glass and various other chalcogenide glasses [47-49].

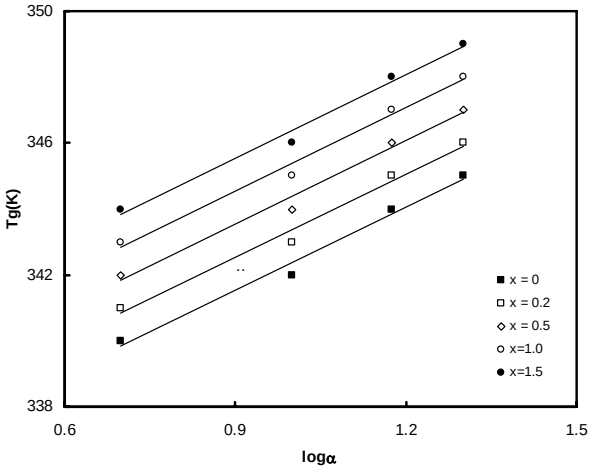

Fig. 5. Variation of T_g with heating rates (α) for $Se_{80-x}Te_{20}Bi_x$ system.

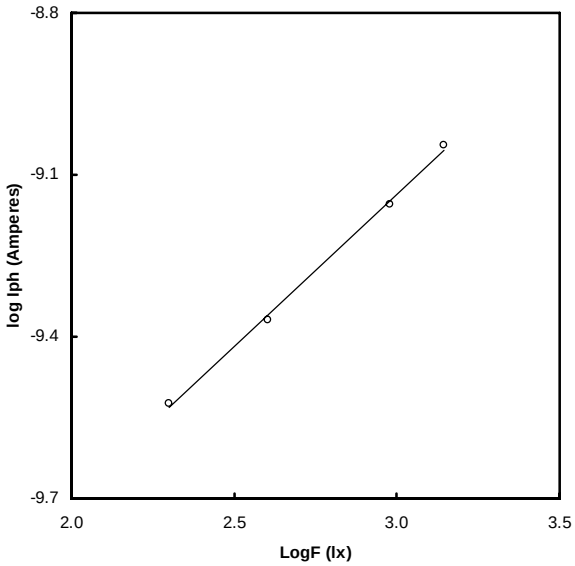

Fig. 6. Variation of photocurrent with light intensity in $Se_{79}Te_{20}Bi_1$ thin films

Table1 Parameters determined from the heating rate dependence of $Se_{80-x}Te_{20}Bi_x$ [3].

X	B	E_t (KJ/mol)	mE_c/n (KJ/mol)	n	m	E_c (KJ/mol)	mE_c (KJ/mol)	E_c (KJ/mol)
0.0	16.61	125.16	97.35	4.05	4	97.35	380.18	95.04
0.2	12.21	185.70	86.06	2.45	2	86.06	267.00	133.50
0.5	11.47	197.00	69.20	2.01	2	69.20	237.00	118.50
1.0	9.74	236.00	63.30	2.30	2	63.30	299.00	149.50
1.5	8.43	272.62	72.14	1.96	1	72.14	247.57	247.57
2.0	4.85	471.00	67.76	2.03	2	67.76	257.00	128.50
4.0	3.75	499.00	56.28	2.10	2	56.28	247.00	123.50
6.0	3.00	508.00	50.10	2.22	2	50.10	230.00	115.00
8.0	2.15	520.00	58.18	2.45	2	58.18	288.00	144.00

The ease in glass formation is determined by calculating the reduced glass transition temperature. The value obtained obey the two-thirds rule which states

$$\frac{T_g}{T_m} = \frac{2}{3} \tag{4}$$

Two-third rule holds well for this composition. The difference between T_c and T_g, which is an indication of the thermal stability of glasses against crystallization decreases with the increase in Bismuth content. This indicates a decrease in the thermal stability of the glass with increase in Bismuth concentration in Se-Te-Bi glass system. The glass forming parameter is calculated using Hruby's parameter [50]

$$K_{gl} = \frac{T_c - T_g}{T_m - T_c} \tag{5}$$

The values of K_{gl} are found to decrease with increasing Bi content. The values of T_c-T_g, K_{gl} and T_{rg} are listed in Table 2.

Table 2. Values of (T_c-T_g), K_{gl} and T_{rg} calculated from DSC thermograms taken at 10 K/min heating rate for $Se_{80-x}Te_{20}Bi_x$ [3].

x	T_g (k)	T_c (k)	T_m (k)	(T_c - T_g)	(T_m- T_c)	K_{gl}	T_{rg}
0.0	337	402	521	65	119	0.54	0.64
0.2	343	389	529	46	140	0.32	0.64
0.5	344	384	530	40	146	0.27	0.64
1.0	345	380	534	35	154	0.22	0.64
1.5	346	375	536	29	161	0.18	0.64
2.0	347	375	531	28	145	0.19	0.60
4.0	349	374	533	25	146	0.17	0.60
6.0	351	371	536	20	156	0.12	0.60
8.0	353	368	538	15	172	0.08	0.60

4.3 Optical Band Gap

In this section, a systematic study of optical properties of thermally evaporated thin films of amorphous $Se_{80-x}Te_{20}Bi_x$ ($0 \le x \le 1$) has been discussed. The values of the band gap energy calculated for different Bismuth concentrations [2] are given in Table 3. From this table it can be seen that the optical band gap decreases with Bismuth concentration. Optical absorption depends upon both the short range order in the amorphous state and the defects associated with it. A decrease in optical band gap in this system may be due to reduction in the amount of disorder in the system and increase in the density of the defect states [51]. The variation of E_g^{opt} follows the same trend as that reported for antimony addition to the Se-Te system [52-53].

4.4 Temperature dependent dark conductivity in Se-Te-Bi system

The conductivity of the samples increases with increase in temperature [2]. Table 3 shows the variation of ΔE_d with Bismuth concentration. It is seen from the table that the activation energy decreases with an increase in Bismuth content. Increase in dark conductivity and decrease in activation energy is associated with the shift in the Fermi level in impurity doped chalcogenide glasses [54-57].

Table3 The variation of optical band gap (E_g^{opt}) and conductivity activation energy in dark (ΔE_d) and in light (ΔE_{ph}) on bismuth content (x) in $Se_{80-x}Te_{20}Bi_x$ (x=0, 0.2, 0.5, 1.0) thin films [2] .

Composition x	Optical bandgap, E_g^{opt} (eV)	Conductivity activation energy	
		In dark, ΔE_d (eV)	In light, ΔE_{ph} (eV)
0.0	1.46	0.73	0.20
0.2	1.41	0.60	0.17
0.5	1.38	0.56	0.16
1.0	1.32	0.50	0.14

4.5 Temperature and intensity dependent photoconductivity in Se-Te-Bi system

The temperature dependence of steady state photoconducticty has been studied in the a-$Se_{80-x}Te_{20}Bi_x$ system in the range 253-333 K. The temperature dependence of photoconductivity at 800 lx for different samples (x = 0.0, 0.2, 0.5, 1.0) has been performed [2]. The variation of photoconductivity with temperature is similar to the variation of the dark conductivity. The values of activation energy in the light (ΔE_{ph}) have been reported in Table 4. It is clear from the table that the activation energy in the light is less than the activation

energy in the dark. The lower activation energy under illumination can be explained by assuming the presence of electron and hole traps in the band gap. In the presence of light, the Fermi level splits into electron and hole quasi-Fermi levels and move towards the conduction band for electrons (E_{Fn}) and towards the valence band for holes (E_{Fp}). The position of the quasi-Fermi level depends on the light intensity [58]. Simmons and Taylor [59] have shown in their theoretical model for photoconductivity that for moderate and intermediate level illumination, the photoconduction is mainly due to holes and the hole concentration in the light, p, is proportional to exp [-(E_2-E_v)/2kT), where E_2 is the energy level of the hole traps near the valence band. They also assumed electron traps at E_1 below the conduction band such that (E_c-E_1) > (E_2-E_v). A model constructed on similar lines for the present $Se_{79}Te_{20}Bi_1$ system [2]. The photocurrent dependence on temperature is same as that of the hole concentration dependence on temperature. It can be seen from the above relation that the photocurrent will be activated with activation energy equal to (E_2-E_v)/2. The variation of photocurrent with light intensity for samples with x = 1.0 is shown in Figure 6. This variation of photocurrent with light intensity obeys the power law

$$I_{ph} = F^{\gamma} \tag{6}$$

where I_{ph} is the photocurrent (total minus dark current), F is the intensity of light and γis the exponent that characterizes the recombination mechanism. In the present case the value of γ calculated from the slope of the figure is 0.5, which shows that the bimolecular recombination process is dominant mechanism [60] that controls the photoconductivity in $Se_{80-x}Te_{20}Bi_x$. In these materials the recombination is between an electron trapped at D^+ and a hole at D^-, which is nothing but the exchange of an electron between two D^0 centers. A value of γ= 0.5 has been predicted by Simmons and Taylor for amorphous semiconductors for moderate light intensities. This value is observed for all the samples.

Table. 4 The variation of optical band gap (E_g^{opt}) and the conductivity activation energy (E_{av}) on bismuth content (x) in as-prepared and annealed $Se_{80-x}Te_{20}Bi_x$ (x = 2, 4, 6, 8) thin films [64].

Bismuth (at%)	E_g^{opt} (eV)		E_{av} (eV)	
(x)	as- prepared	annealed	as- prepared	Annealed
2	1.30	1.28	0.106	0.081
4	1.24	1.20	0.090	0.065
6	1.21	1.11	0.076	0.043
8	0.97	0.87	0.062	0.041

4.6 Annealing effects on optical properties of Se-Te-Bi system

In order to determine the absorption coefficient αof the films versus the incident energy, transmission T (λ) measurements were carried out at room temperature. The linear relation of the $(\alpha h\nu)^{1/2}$ vs. (hνplot indicates that the absorption mechanism in this system is a non-direct transition. The optical band gap for non-direct transition can be obtained by the intercept of the above plots with the energy axis at $(\alpha h\nu)^{1/2}= 0$. The optical band gap decreases from 1.30 to 0.97 in as-prepared thin films. Increasing the Bi content causes an increase in the density of states in the valence band. On the other hand, the increase in the Bi content creates the localized states in the band gap [61]. The decrease in the optical band gap of annealed films from 0.081 to 0.041 as the Bismuth content x is increased from 2 to 8 is due to the rearrangement of localized defect states, D^+ and D^- [62].

4.7 Annealing effects on electrical studies of Se-Te-Bi system

The DC conductivity measurements yield valuable information about the conduction mechanism in amorphous semiconductors. Chalcogenide glasses normally show an activated temperature dependent dark conductivity.

The dark conductivity of the samples increases with the increase in the temperature [63]. The activation energy decreases with the increase in Bismuth content as seen from Table 4 for as-prepared samples. This increase in the conductivity and decrease in the activation energy is due to movement of Fermi level (E_F) towards the conduction band and hence the origin of extrinsic n-type semiconductor. The activation energy (Table 4) has substantial decrease when the samples are annealed below glass transition temperature. Thermal annealing seems to re-adjust the localized states in such a way that there is substantial decrease in the value of ΔE.

5. Summary

In this paper we have reviewed the most striking experimental results obtained while studying the effect of Bismuth addition on Se-Te chalcogenide system. The results were discussed on the basis of defects and disorder present in chalcogenide system. A model for photoconductivity of samples was presented for Se-Te:Bi system on the basis of Simmons and Taylor model for photoconductivity.

From overall review we come to the conclusion that a little more work should be done in order to understand the effect of Bismuth on chalcogenide glasses. X-ray absorption near edge structure (XANES) can be performed for better understanding of the local structure. Differential Scanning Calorimetry studies for higher heating rates (up to 100 K/min) is essential in order to have a better

understanding of the dependence of T_g and T_p on heating rates.

Acknowledgements

The authors wish to thank all the members of the Hybrid microcircuits group for their support and to the Director CEERI for his encouragement and permission to publish the results.

References

[1] N. F. Mott, E. A. Davis Electronic Processes in Non-crystalline Materials, second edition, Oxford University (1979**).**
[2] N. Suri, K.S. Bindra, R. Thangaraj, J. Phys.: Condens. Matter **18**, 9129 (2006).
[3] N. Suri, K.S. Bindra, P. Kumar, M.S. Kamboj, R. Thangaraj, J. Ovonic, Research **2**, 111 (2006).
[4] S. A. Fayek, M. El-Ocker, A.S. Hassanien, J. Mater. Res. **16**, 1549 (2001).
[5] R. Chiba, N. Funakoshi, J. Non-Cryst. Solids 105, 149 (1988).
[6] N. Toghe, Y. Yamamoto, T. Minami, M. Tanaka, J. Appl. Phys. Lett. **34**, 640 (1979).
[7] N. Toghe, T. Minami, M. Tanaka, J. Non-Cryst. Solids **59–60**, 999 (1983).
[8] P. Nagels, M. Rotti, W. Vikhrov, J. Phys. (Paris) **42**, 907 (1981).
[9] P. Nagels, L. Tichy, A. Tiska, H. Ticha, J. Non-Cryst. Solids **59–60**, 1015 (1983).
[10] J. C. Schottmiller, D. Bowman, C Land Wood, J . Appl. Phys. **39**, 1663 (1968).
[11] Z. Wang, C. Tu, Y. Li, Q. Chen, J. Non-Cryst. Solids **191**, 132 (1995).
[12] H. El-Zahed, A. El-Korashy, Thin Solid Films **376**, 236 (2000).
[13] A. El-Korashy, N. El-Kabany, H. El-Zahed, Physics B **365**, 55 (2005).
[14] H. El-Zahed, A. El-Korashy, Thin solid films **376**, 236 (2000).
[15] P. Sharma, M. Vashistha, I. P Jain, J. Optelectron. Adv. Mater. **7**, 2647 (2005).
[16] Z. H Khan, M. Zulfequar, M. Husain, J. Modern Optics **44**, 1 (1997)
[17] O. EL- Shazly, M. M. Hafiz, Journal Mat. Sci. **12**, 395 (2001).
[18] A. K. Agnihotri, A. Kumar, A.N. Nigam, J. Non-Cryst. Solids **93**, 267 (1987).
[19] A. K. Agnihotri, A. Kumar, A. N. Nigam, Phil. Mag. B **57**, 319 (1988).
[20] S. R. Elliot, A. T. Steel, J. Phys. C: Solid State Phys. **20**, 4335 (1987).
[21] H. Fritzsche, M. Kastner, Phil. Mag. B **37**(3), 285 (1978).
[22] N. Asha Bhat, K. S. Sangunni, K. S. R. K. Rao, J. Optoelectron. Adv. Mater. **3** 735 (2001).
[23] Y. Wang, E. Ohata, S. Hosokawa, M. Sakurai, E. Matsubara, J. Non-Cryst.Solids, **337**, 54 (2004).
[24] D.A. Turnbull, J. S. Sanghera, V. Q. Nguyen, I. D. Aggarwal, Mat. Lett. **58**, 51 (2003).
[25] S. R. Elliott, Physics of Amorphous Materials, Longman Scientific & Technical & John Wiely & Sons, New York,(1990)
[26] M. Mitkova, M. N. Kozicki, H. C. Kim, T. L. Alford, J. Non-Cryst. Solids **338,** 552 (2004).
[27] M. Dongol, M. Abou Zied, G. A. Gamal, A. EI-Denglawey, Physica B: Condensed Matter **353**, 169 (2004).
[28] V. I. Verlan, J. Optoelectron. Adv. Mater. **5**, 1121 (2003).
[29] A. K. Pattanaik , A. Srinivasan, Semicond. Sci. Tech. **19**, 157 (2004).
[30] M. S. Kamboj, G. Gaur, R. Thangaraj, D. K. Avasthi, J. Phys. D: Appl. Phys. **35**, 477 (2002).
[31] G. H. Chandra, O. M. Hussain, S. Uthanna, B. S. Naidu, Vacuum **62**, 39 (2001).
[32] V. Balan, C. Vigreux, A. Pradel, J. Optoelectron. Adv. Mater. **6**, 875 (2004).
[33] M. D. Mikhailov, I. I. Kryzhanowsky, I. M. Petcherizin, J. Non-Cryst. Solids 265, 1 (2000).
[34] M. G. Sandoval-Paz, M. Sotelo-Lerma, J. J. Valenzuela-Juregui, M. Flores-Acosta, R. Ramrez-Bon, Thin Solid Films **472**, 5 (2005).
[35] P. Nagels, R. Mertens, L. Tichy, Mat. Lett. **57**, 2494 (2003).
[36] J. Thurn, R. F. Cook, M. Kamarajugadda, S. P. Bozeman, L. C. Stearns, J. Appl. Phys. **95**, 967 (2004).
[37] S.O.Kasap, T.Wagner, V.Aiyah, O.Krylouk, A.Bekirov, L.Tichy, J.Mat. Sci, **34**, 3779 (1999).
[38] J. Tauc, Amorphous and Liquid Semiconductors, Plenum, New York 569 (1974).
[39] M. M. A. Imran, D. Bhandari, N. S. Saxena, Physica B **293**, 394 (2001).
[40] P. Agarwal, S. Goel, J. S. P. Rai, A. Kumar, Phys Stat Sol (a) **127**, 363 (1991).
[41] L. Tichy, N. Rysava, A. Trisk, H. Ticha, A. Klikorka, J. Solid Stat Comm **49**, 903 (1984).
[42] H. E. Kissinger, J. Res Mat. Bur. Stand. **57**, 217 (1956).
[43] K. Matusita, S. Saka, Phys. Chem. Glasses **20**, 81 (1979).
[44] D. R. Macfarane, M. Maecki, M. Poulain, J. Non-Cryst. Solids **64**, 351 (1984).
[45] K. Matusita, T. Komatsu, R. Yokata, J. Mater. Sci. **19**, 291 (1984).
[46] H. S. Chen, J. Non-Cryst Solids **27,** 257 (1978).
[47] M. S. Kamboj, R. Thangaraj, Eur. Phys. J. App. Phys. **24**, 33 (2003)
[48] G. Kaur, T. Komatsu, R. Thangaraj, J. Mater. Sci. **35**, 903 (2000).
[49] G. Kaur, T. Komatsu, J. Mater. Sci. **36,** 4530 (2001).
[50] A. Hruby , Czech J. Phys B **22,** 1187 (1972).
[51] Z. H Khan, M. Zulfequar, M. Hussain J. Mod. Opt. **44**, 55 (1997).
[52] R. M. Mehra, G. Kaur, A. Ganjoo, R. Singh, P. C. Mathur Phys. Status Solidi a **124**, K51 (1991).
[53] M. S. Kamboj, G. Kaur, R. Thangaraj Thin Solid

Films **350**, 420 (2002).
[54] B. T. Kolomiets, E. A. Lebedex, N. A. Rogachov ,Fiz. Tekh. Poluprov. **8**, 545 (1974).
[55] S. Koichi, Y. Akaira, A.Tatsuya, J. Non-Cryst. Solids **16**, 258 (1974).
[56] E. A Davis, N. F. Mott Phil. Mag. **22**, 903 (1970).
[57] R. A Street, Phys. Rev. Lett. **49**, 1187 (1982).
[58] S. Singh, R. S. Sharma, R. K. Shukla, A. Kumar Vacuum **72**, 1 (2003).
[59] J. G. Simmons, G. W. Taylor, J. Phys. C: Solid State Phys. **7**, 3051 (1974).
[60] R. H. Bube, "Photoconductivity of Solids" (Wiley & Sons, New York, 1960).
[61] N. Barreau, S. Marsillac, J. C. Bernede, T. Ben Nasrallah, S. Belgacem, Phys. Status Solidi (a) **184**, 179 (2001).
[62] N. F Mott, E. A Davis, R. A .Street, Phil. Mag. **36**, 961 (1975).
[63] N.Suri, K.S.Bindra, M.Ahmad, J.Kumar, R.Thangaraj, Appl. Phys.A **90**, 149 (2008).

*Corresponding author: surinikhil@rediffmail.com